

^{133}Cs and ^{35}Cl NMR spectroscopy and molecular dynamics modeling of Cs^+ and Cl^- complexation with natural organic matter

Xiang Xu, Andrey G. Kalinichev, R. James Kirkpatrick *

Department of Geology and NSF WaterCAMPWS, University of Illinois at Urbana-Champaign, Urbana, IL 61801, USA

Received 23 January 2006; accepted in revised form 5 June 2006

Abstract

Interaction of dissolved aqueous species with natural organic matter (NOM) is thought to be important in sequestering some species and enhancing the transport of others, but little is known about these interactions on a molecular scale. This paper describes a combined experimental ^{133}Cs and ^{35}Cl nuclear magnetic resonance (NMR) and computational molecular dynamics (MD) modeling study of the interaction of Cs^+ and Cl^- with Suwannee River NOM. The results provide a detailed picture of the molecular-scale structure and dynamics of these interactions. Individual NOM molecules are typically hundreds to thousands of Daltons in weight, and on the molecular scale their interaction with small dissolved species can be investigated in ways similar to those used to study the interaction of dissolved aqueous species with mineral surfaces. As for such surface interactions, understanding both the structural environments and the dynamics over a wide range of frequencies is essential. The NMR results show that Cs^+ is associated with NOM at pH values from 3.4 ± 0.5 (unbuffered Suwannee River NOM solution) to 9.0 ± 0.5 . The extent of interaction increases with decreasing CsCl concentration at constant pH. It also decreases with increasing pH at constant CsCl concentration due to pH-dependent negative structural charge development on the NOM caused by progressive deprotonation of carboxylic and phenolic groups. The presence of NOM has little effect on the ^{133}Cs chemical shifts, demonstrating that its local coordination environment does not change significantly due to interaction with the NOM. Narrow, solution-like line widths indicate rapid exchange of Cs^+ between the NOM and bulk solution at frequencies of $>10^2$ Hz. The MD simulations support these results and show that Cs^+ is associated with the NOM principally as outer sphere complexes and that this interaction does not reduce the Cs^+ diffusion coefficient sufficiently to cause NMR line broadening. The ^{35}Cl NMR data and the MD results are consistent in demonstrating that there is no significant complexation between Cl^- and NOM in the pH range investigated, consistent with negative structural charge on the NOM.

© 2006 Elsevier Inc. All rights reserved.

1. Introduction

Natural organic matter (NOM) is ubiquitous in the environment and plays a variety of important geochemical roles including acting as a proton donor/acceptor and pH buffer and interacting with metal ions, minerals and organic species to form water-soluble and water-insoluble complexes of widely differing chemical and biological stabilities (Aiken et al., 1985; Buffle, 1988; Struyk and Sposito, 2001). There are strong correlations among the

concentration of natural organic matter and the speciation, solubility and toxicity of many trace metals due to metal–NOM interaction (Sposito, 1981; Buffle, 1988; Hamilton-Taylor et al., 2002). NOM also plays a significant negative role by causing bio-fouling of nanofiltration and reverse osmosis membranes used industrially for water purification and desalination (e.g., Hong and Elimelech, 1997; Lee et al., 2005). The molecular scale mechanisms and dynamics of the interaction of NOM with metals and membranes are, however, poorly understood. This paper presents a combined experimental ^{133}Cs and ^{35}Cl nuclear magnetic resonance (NMR) and computational molecular dynamics (MD) modeling study that advances understanding of the solute–NOM interaction at the molecular scale.

* Corresponding author.

E-mail address: kirkpat@uiuc.edu (R.J. Kirkpatrick).

NOM is compositionally and structurally complex and heterogeneous, and NOM samples from different locations often have significantly different structures and compositions. It is normally not possible to define a unique structure, even for NOM from one locality. The reported apparent molecular weights range from a few hundred to several hundred thousand Daltons (e.g., Perminova et al., 2003). Whether NOM molecules are single macromolecular entities or supramolecular assemblages of smaller molecules held together by relatively weak attractive forces is still under discussion (Swift, 1999; Wershaw, 1999; Haynes and Clapp, 2001; Piccolo, 2001; Leenheer and Croué, 2003). The most recent experimental evidence seems to support the latter view (Simpson et al., 2002; Peña-Méndez et al., 2005). These uncertainties contribute to the difficulty in characterizing metal–NOM binding in molecular-scale detail. It is known that the extent of binding varies with the size, composition and configuration of the NOM, the pH and the ionic strength of the solution, the chemical properties of the metal, and the metal/NOM compositional ratio (Buffle, 1988; Li et al., 1998; Myneni et al., 1999; Elkins and Nelson, 2002; Huber et al., 2002; Tipping et al., 2002; Pullin and Cabaniss, 2003; Ritchie and Perdue, 2003). Previous sorption studies of metal–NOM binding have provided important, quantitative potentiometric titration data and ion absorption isotherms (Sposito, 1981; Oliver et al., 1983; Buffle, 1988; Gaffney et al., 1996; Leenheer et al., 1998; Li et al., 1998; Davies et al., 2001; Elkins and Nelson, 2002; Hamilton-Taylor et al., 2002; Tipping et al., 2002; Ritchie and Perdue, 2003). These experiments, however, do not directly probe molecular scale interactions and, thus, do not provide information about the structure, dynamics, and chemical mechanisms of interaction. ^{13}C and ^1H NMR and FT-IR spectroscopic studies of Ca^{2+} -, Cd^{2+} -, Cu^{2+} -, Ni^{2+} -, and Zn^{2+} -exchanged fulvic acid (FA) isolated from Suwannee River NOM, however, have suggested that metals are bound to FA in different ways (Leenheer et al., 1998). The results suggest, for instance, that Ca^{2+} is coordinated to the FA carboxylic groups as inner sphere complexes, whereas Cd^{2+} occurs as outer sphere complexes associated with the quinone carbonyl groups. ^{13}C , ^1H , and ^1H - ^{13}C CP/MAS NMR are also commonly used to probe NOM structure and provide important quantitative information about the carbon content and functional groups (Mao et al., 2000; Wershaw et al., 2000; Conte et al., 2002; Kaiser, 2003; Ritchie and Perdue, 2003).

There have been fewer studies of NOM behavior using the NMR properties of the solute species. ^{113}Cd NMR chemical shifts combined with titration data show that Cd^{2+} complexation with Suwannee River NOM occurs primarily with carboxylic groups at Cd/C ratios of 0.001–0.007 and pH 3–9. The $^{113}\text{Cd}^{2+}$ peak widths increase with increasing pH, suggesting that the Cd–NOM exchange rates are higher at acidic conditions than at higher pHs (Li et al., 1998). For ^{51}V , the NMR chemical shifts vary significantly with pH and concentration, indicating interac-

tion of a variety of vanadate and poly-vanadate ions with aquatic humic substances (Lu et al., 1998).

Similarly, despite decades of widespread use of computational molecular dynamics (MD) and Monte Carlo (MC) methods (e.g., Allen and Tildesley, 1987; Cygan and Kubicki, 2001; Schlick, 2002), these techniques have been rarely applied to the investigation of NOM and its interaction with aqueous solutions and mineral surfaces (Schulten and Schnitzer, 1997; Leenheer et al., 1998; Kubicki and Apitz, 1999; Sein et al., 1999; Shevchenko et al., 1999; Diallo et al., 2003; Porquet et al., 2003; Sutton et al., 2005). Classical molecular computer simulations are typically performed for systems containing 10^3 – 10^6 particles (atoms, ions, and/or molecules) and can thus effectively capture longer range and cooperative behavior of the simulated systems. Using standard statistical mechanics formalism to analyze the large number of computed instantaneous molecular configurations (e.g., Allen and Tildesley, 1987), these methods can yield many important thermodynamic, structural, spectroscopic, and transport properties. Molecular modeling of NOM is complicated by the lack of well-defined compositions and structures for the NOM molecules (e.g., Sein et al., 1999; Diallo et al., 2003; Leenheer and Croué, 2003). Nevertheless, the principal functional groups of many NOMs are known (Ritchie and Perdue, 2003), and previously proposed structural models for NOM molecules (Sein et al., 1999) allow for their effective MD modeling.

This paper describes a combined NMR and MD study of the interaction of Cs^+ and Cl^- with NOM in aqueous solution. The results show that the ability of combined NMR and MD studies to effectively probe molecular-scale structure and dynamics at solution–solid interfaces (Weiss et al., 1990; Kim et al., 1996b; Kim and Kirkpatrick, 1997, 1998; Yu and Kirkpatrick, 2001; Rossi et al., 2003) can be extended to NOM in solution. Experimentally, ^{133}Cs and ^{35}Cl NMR chemical shift, line width, and $1/T_1$ relaxation rate data for solutions containing Cs^+ , Cl^- , and Suwannee River NOM (SRNOM) were obtained to explore both the structural and dynamical aspects of the interactions. SRNOM was chosen for the study, because its composition is relatively well characterized (Aiken et al., 1994; Wagoner and Christman, 1997). ^{137}Cs is an important and abundant component of many nuclear waste streams. It is one of the most hazardous radionuclides in the environment because of its high mobility, strong γ -emission, relatively long half-life ($t_{1/2} = 30.17$ years), and high solubility (Walling and Quine, 1991; Ruhm et al., 1999; Bunzl et al., 2001; Hinton et al., 2001). Previous research has shown a strong and direct effect of organic matter on Cs fixation (Tegen et al., 1991; Thiry and Myttenaere, 1993; Valcke and Cremers, 1994), but the mechanisms are unknown. From an NMR perspective, ^{133}Cs is readily observed with relatively high sensitivity. It has a 100% natural abundance and a small electric quadrupolar moment ($Q = -3 \times 10^{-31} \text{ m}^2$), resulting in quite narrow solid state line widths. Previous ^{133}Cs NMR

studies of Cs⁺ adsorption onto clay minerals including kaolinite and illite have shown that NMR is an effective tool to investigate its adsorption sites and atomic-scale dynamics on mineral surfaces (Weiss et al., 1990; Kim et al., 1996a,b; Kim and Kirkpatrick, 1997, 1998). The results have shown that Cs⁺ is adsorbed on mineral surfaces both by direct coordination to the surface (inner sphere complexes) and more loosely as outer sphere complexes and in the diffuse layer. ³⁵Cl NMR has also been shown to be an effective probe of the structure and dynamics of surface-associated Cl⁻ (Kirkpatrick et al., 1999; Yu and Kirkpatrick, 2001).

2. Methods

2.1. Materials and sample preparation

The SRNOM was purchased from the International Humic Substances Society (Cat. No. 1R101N). It was originally collected from the Suwannee River in Georgia, USA, and was purified using reverse osmosis (Ritchie and Perdue, 2003). Its elemental composition (wt %) is C 52.47%, H 4.19%, O 42.69%, N 1.10%, S 0.65%, and P 0.02% (Ritchie and Perdue, 2003). The major acid sites estimated from titration data are carboxylic groups: 9.85 mol/kgC and phenolic groups: 3.94 mol/kgC (Ritchie and Perdue, 2003).

NMR data were collected for two sets of CsCl–NOM solution samples. The objective of *sample set I* was to evaluate the concentration dependence of Cs⁺ and Cl⁻ complexation with SRNOM at the natural pH of our NOM solution near 3.4. These solutions were prepared by first dissolving the NOM in MilliQ water at a fixed concentration of 0.6 mg/ml and then adding the desired amount of solid CsCl to 2 ml of the 0.6 mg/ml NOM solution in a 10 mm glass NMR tube. After the CsCl dissolved, MilliQ water was added to make a total solution volume of 3 ml. The NOM/CsCl ratios were, thus, controlled by varying the CsCl concentrations from 0.0001 to 4 M at a fixed NOM concentration of 0.4 mg/ml. No background electrolyte was used. The pH values of these CsCl–NOM mixtures were all 3.4 ± 0.5. Reference neat CsCl solutions were also made with concentrations ranging from 0.0001 to 4 M. The pH values of these samples were all 7.0 ± 0.5. The objective of *sample set II* was to investigate the effect of pH on Cs⁺ and Cl⁻ association with NOM. Samples were prepared using the methods described above. HCl and CsOH were then added to adjust the pHs of the CsCl–NOM and neat CsCl solutions to values of 3.4 ± 0.5, 7.0 ± 0.5, and 9.0 ± 0.5, with Cs⁺ concentrations varying from 0.001 to 1 M.

2.2. ¹³³Cs and ³⁵Cl NMR measurements

The ¹³³Cs and ³⁵Cl NMR data for *sample set I* were collected with a Varian UNITY INOVA™ 500WB NMR spectrometer and the data for *sample set II* with a Varian

UNITY INOVA™ 600WB NMR spectrometer. Both systems were controlled by a SUN SPARCstation 5 computer via a Varian VNMR software overlay. In all cases, freshly prepared samples were held in 10 mm NMR tubes at a fixed temperature of 22 °C and were examined without probe spinning. A phase cycled, single pulse sequence was used to obtain ¹³³Cs and ³⁵Cl chemical shifts. Typical parameters for ¹³³Cs were: spectral width 70 ppm, pulse width 14.4–22.9 μs (90° pulse angle), and recycle time 60 s. For ³⁵Cl these were: spectral width 70 ppm, pulse width 15.5–22.1 μs (90° pulse angle), and recycle time 0.3 s. A standard inversion-recovery pulse sequence (180°–τ–90°–acquire) was used for T₁ measurements. Depending on CsCl concentration, between 2 and 516 scans were collected for both nuclei. A 10 Hz line broadening was performed on the free induction decays before Fourier transformation. All the chemical shifts were externally referenced to a 1 M CsCl solution standard, which was assigned to 0 ppm for both ¹³³Cs and ³⁵Cl. The chemical shift of D₂O used for the deuterium frequency lock was used as a secondary reference. Several CsCl–NOM samples at pH 3.4 ± 0.5 and neat solutions at pH 7.0 ± 0.5 from *sample set I* were examined using both the 500WB and 600WB NMR spectrometers. In all cases, the chemical shifts and T₁ values at the two fields are identical to within experimental error and it is, thus, acceptable to compare data from the two instruments.

2.3. Molecular modeling methods

The “Steelink” and “Temple-Northeastern-Birmingham” (TNB) models of humic acid monomers (Sein et al., 1999) were used in our simulations. Preliminary MD simulations for NOM–CsCl aqueous solutions were performed for both models, but most of the production MD runs used the TNB model, because its C/O/H ratio corresponds slightly better to that of SRNOM (Table 1). Both models have 3 carboxylic groups, 3 carbonyl groups, 2 phenolic groups, and 4 other R–OH alcohol groups. The TNB model also has 2 amine groups, while the Steelink model has only one. The molecular weight of the TNB model is 753 Daltons, which is within the range of the most frequently occurring NOM molecules (Simpson et al., 2002; Peña-Méndez et al., 2005).

For the simulations, we assume that the carboxylic groups of NOM are fully deprotonated and the phenolic groups are fully protonated, thus simulating near-neutral pH conditions. The –3 charge of the resulting NOM anion was compensated by adding 3 initial Cs⁺ ions, and this system was hydrated by 556 water molecules in a cubic MD simulation box with periodic boundary conditions (e.g., Allen and Tildesley, 1987; Schlick, 2002). More concentrated NOM–CsCl solutions were created by randomly substituting Cs⁺ and Cl⁻ for some of the H₂O molecules. Neat CsCl aqueous solutions of the same concentrations were simulated for comparison. A total of 16 MD simulations were performed covering the concentration range from 0.1 to 4.0 M

Table 1
Compositions of NOM building blocks according to the two models used in the MD simulations

	C (wt %)	H (wt %)	O (wt %)	N (wt %)	S (wt %)	P (wt %)	Carboxyl (mol/kgC)	Phenolic (mol/kgC)
Stealink ^a	59.5	5.2	33.5	1.8	—	—	6.6	4.4
TNB ^a	57.4	4.9	34.0	3.7	—	—	7.0	4.5
Exp. (SR) ^b	52.5	4.2	42.7	1.1	0.6	0.02	9.85	3.94

^a Sein et al. (1999).

^b Experimental data for Suwannee River NOM (Ritchie and Perdue, 2003).

for both neat and NOM containing solutions. Fig. 1 illustrates the size and composition of the simulated systems.

The widely used simple point charge (SPC) potential (Berendsen et al., 1981) was applied in our simulations to describe the intermolecular interactions of water molecules. The SPC-compatible parameters for Cs^+ - H_2O and Cl^- - H_2O interactions were taken from the literature (Dang and Smith, 1993; Dang, 1995). The interactions of NOM molecules with aqueous species were described using the consistent valence force field (CVFF; Kitson and Hagler, 1988), which is also consistent with the SPC water model. Long-range electrostatic contributions to the intermolecular potential energy in the simulated systems were calculated

using an Ewald summation algorithm, and a “spline cutoff” method was applied to the short-range van der Waals interactions (e.g., Allen and Tildesley, 1987). The MD time step was 1.0 fs. To assure proper thermodynamic equilibration and NOM conformational relaxation of the initial models, pre-equilibration MD runs were performed for all simulated systems in several stages. First, a constant-volume (*NVT*-ensemble) MD simulation was run for 20 ps at a high temperature of 600 K. Then the temperature was decreased in 50 K steps with similar MD equilibration at each step until the system was brought to 300 K. At this temperature an additional 20 ps pre-equilibration MD run was performed at a constant pressure of 1 bar

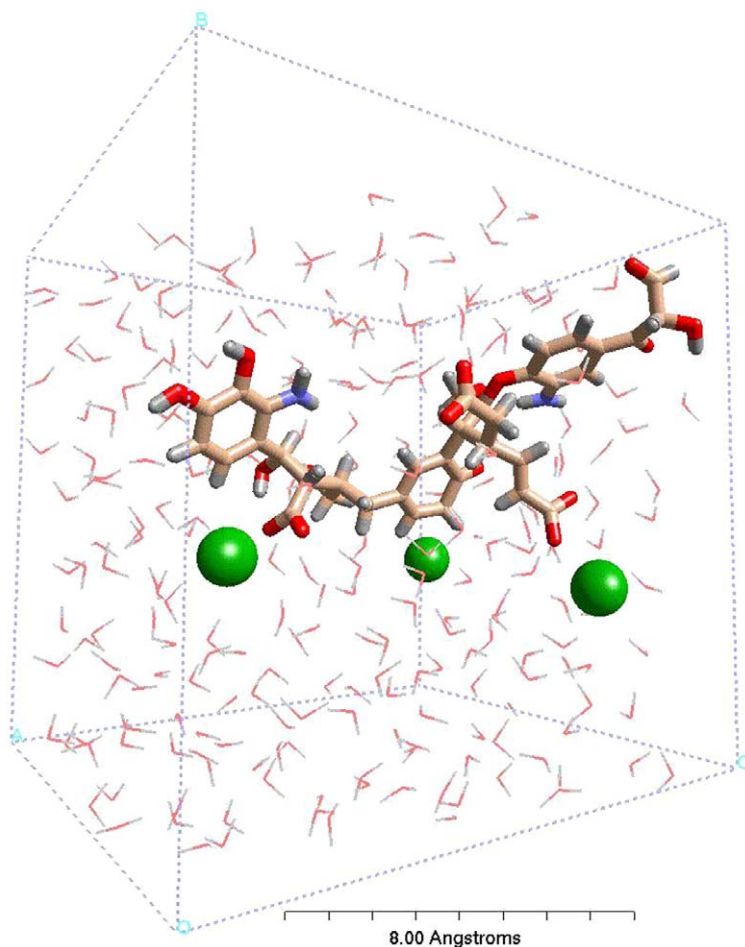


Fig. 1. A snapshot of the MD simulation box containing the NOM model (Sein et al., 1999) in 0.3 M Cs^+ aqueous solution. Carbon atoms of NOM are colored light brown, oxygen atoms are red, hydrogen atoms are gray, nitrogen atoms are blue, and green balls are Cs^+ ions in the outer-sphere coordination to NOM carboxylic groups (left and right) and in the bulk aqueous solution (back, middle). Some water molecules are removed for clarity.

using the standard *NPT*-ensemble MD algorithm (e.g., Allen and Tildesley, 1987). These optimized models were used as the starting configurations for the production MD simulation runs which were all performed in the *NVT*-ensemble at 300 K. Each system was allowed to equilibrate for an additional 20 ps before its equilibrium dynamic trajectory was recorded over the final 100 ps of MD simulation at 10 fs intervals for statistical analysis. For the neat aqueous CsCl solutions, the volume of the MD simulation box at each concentration was initially adjusted to reproduce the experimentally known solution densities under ambient conditions (Lide, 2004). In these simulations, a 50 ps pre-equilibration preceded each 100 ps production run of *NVT*-ensemble MD simulation.

To assess the effects of NOM on the structural environments, diffusion, and vibrational behavior of Cs⁺, we calculated the radial distribution functions (RDFs), running coordination numbers, diffusion coefficients, and power spectra of molecular motions in the solution using standard procedures (e.g., Allen and Tildesley, 1987). The running coordination numbers, $n_{ij}(r)$, were calculated from the RDFs as

$$n_{ij}(r) = 4\pi\rho_j \int_0^{r_{\max}} g_{ij}(r)r^2 dr, \quad (1)$$

where the index i corresponds to Cs⁺ ions, index j to all other species in solution to which Cs⁺ can coordinate, ρ_j is the number density of species j in the system, r_{\max} is the cutoff radius defining the size of the coordination shell, and $g_{ij}(r)$ are the atom–atom RDFs. Based on the computed positions of the Cs⁺ RDF minima, we define the radii of the first and second coordination shells around Cs⁺ as $r'_{\max} = 3.9\text{Å}$ and $r''_{\max} = 6.8\text{Å}$. The diffusion coefficients of all species were calculated from their mean-square displacements. The power spectra of low-frequency dynamics of Cs⁺ and other solution species were calculated as Fourier transforms of the corresponding atomic velocity autocorrelation functions, in a manner similar to the one we used earlier to calculate the vibrational spectra of interlayer and surface species of layered double hydroxides (Kalinichev and Kirkpatrick, 2002; Wang et al., 2003; Kirkpatrick et al., 2005).

3. Results and interpretation

3.1. ¹³³Cs and ³⁵Cl NMR T_1 data and spectral characteristics

The ¹³³Cs $1/T_1$ relaxation rates of CsCl–NOM mixtures increase dramatically with decreasing [Cs]/[NOM] ratio, but are essentially constant for the neat CsCl solutions at all pH values (Fig. 2). For the CsCl–NOM mixtures, the $1/T_1$ values increase with increasing pH at constant [Cs] and increase with decreasing [Cs] at constant pH. At [Cs] greater than about 1 M, they all converge to a value of 0.082 Hz, which is essentially identical to the value for neat solutions (0.084 Hz). At pH 3.4 ± 0.5 , maximum observed $1/T_1$ is approximately three times larger at low concentra-

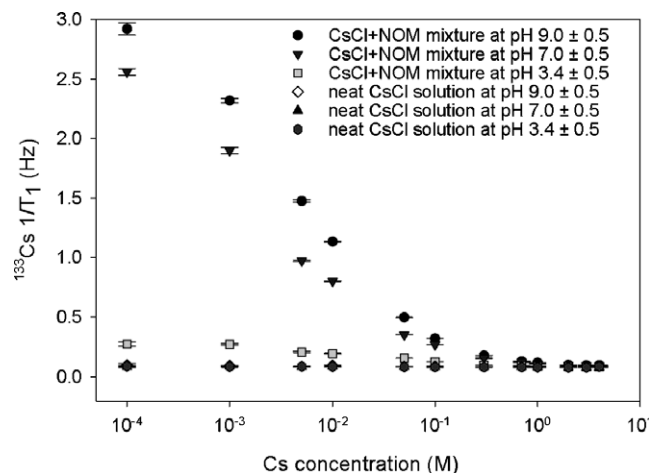


Fig. 2. ¹³³Cs $1/T_1$ relaxation rates of CsCl–NOM mixtures at pH = 3.4 ± 0.5 , 7.0 ± 0.5 , and 9.0 ± 0.5 increase with decreasing [Cs]/[NOM] ratio, whereas they remain essentially constant for neat CsCl solutions. Data for the neat solutions at all pH values plot on top of each other in this diagram.

tions ([Cs] = 0.0001 M) than at high concentrations ([Cs] = 4 M), and at pH 7.0 ± 0.5 and 9.0 ± 0.5 , the largest values (2.921 and 2.560 Hz, respectively) are about 30 times larger than at high concentrations. The $1/T_1$ values for the CsCl–NOM mixtures do not converge to a constant value at low [Cs].

The ¹³³Cs full-widths at half-height (FWHH) of the CsCl–NOM mixtures parallel the $1/T_1$ relaxation rates, decreasing with increasing [Cs] from a maximum of about 20 Hz at low [Cs] to 10 Hz at high concentrations (data not shown). For the neat solutions they are essentially constant at about 10 Hz. There is no significant or systematic variation in the total ¹³³Cs NMR signal intensity with varying [Cs]. This contrasts with the situation for vanadate–NOM interaction, for which quadrupolar line broadening causes loss of signal for NOM–V⁵⁺ complexes that are rigidly bound to the humic substances (Lu et al., 1998). Thus, there is no “missing” Cs in our samples that needs to be accounted for.

The ¹³³Cs NMR spectra of the neat CsCl and CsCl–NOM solutions at all pH values examined contain only a single, narrow resonance, and the chemical shift becomes less shielded (more positive) with increasing CsCl concentration (Figs. 3 and 4). The chemical shifts do not depend on pH or the presence or absence of NOM, except at high Cs concentrations ([Cs] = 2, 3, and 4 M). In this concentration range, the chemical shifts of the CsCl–NOM mixtures are less positive than those of the neat solutions, and at [Cs] = 4 M, the difference increases with increasing pH. The systematic dependence of the ¹³³Cs chemical shifts on [Cs] is well-known (Halliday et al., 1969; Weiss et al., 1990) and is due to the effects of next-nearest neighbor structure on the Cs⁺ electronic environment (Halliday et al., 1969; Fukushima and Roeder, 1981; Akitt, 1989). The observed differences between the neat solutions and the CsCl–NOM mixtures at high [Cs] are not understood,

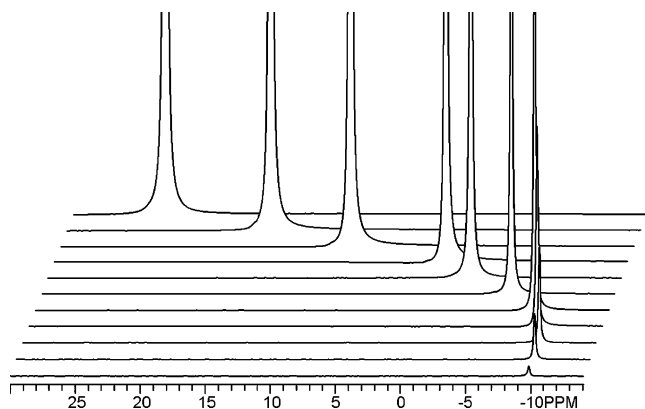


Fig. 3. Static ^{133}Cs NMR spectra of CsCl–NOM mixtures at $\text{pH} = 3.4 \pm 0.5$ (stacked plots are arranged by concentration, decreasing from 4 to 0.0001 M from top to bottom). These spectra are representative of all ^{133}Cs spectra obtained in this study.

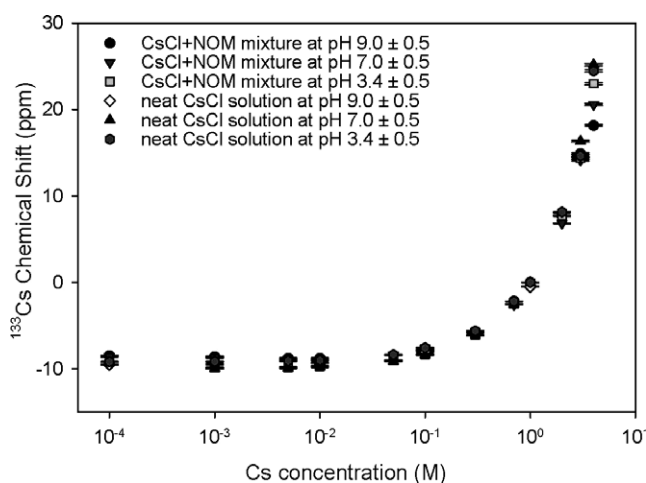


Fig. 4. ^{133}Cs NMR shifts of CsCl solutions and CsCl–NOM mixtures become less shielded with increasing CsCl concentration.

but may be due to NOM effects on direct $\text{Cs}^+ - \text{Cl}^-$ interionic contact, which is not significant at low concentrations. The model of Halliday et al. (1969) for the chemical shifts of neat solutions is known to fail at high concentrations, but our MD simulations seem to support this hypothesis (see discussion below).

The ^{35}Cl NMR spectra of the neat CsCl and CsCl–NOM solutions contain only one narrow, solution-like peak, and the FWHH varies from 17 to 29 Hz with increasing concentration. As for ^{133}Cs , the ^{35}Cl chemical shifts become more positive (less shielded) with increasing CsCl concentration, and there are no differences between the chemical shifts of the neat solutions and CsCl–NOM mixtures at all pH values examined except at $[\text{Cs}] = 3$ and 4 M (Fig. 5). Again, the origin of the differences at high $[\text{Cs}]$ is unknown but may be an effect of NOM on short-range ion–solvent and ion–ion interactions (Halliday et al., 1969). In contrast to ^{133}Cs , however, the ^{35}Cl $1/T_1$ relaxation rates of the neat and CsCl–NOM solutions are identical within experimental error (Fig. 6).

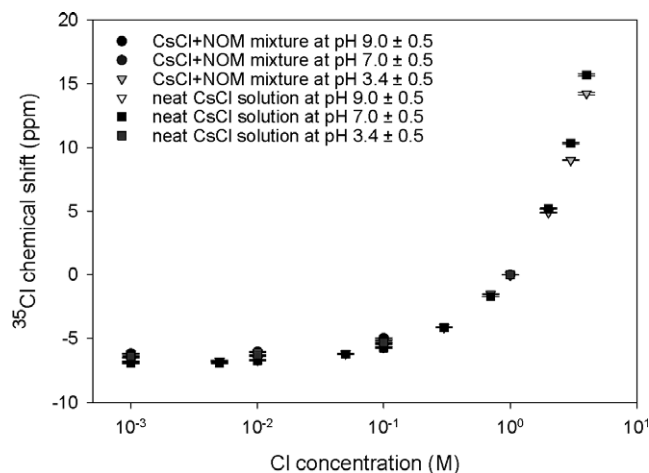


Fig. 5. ^{35}Cl NMR chemical shifts of neat CsCl solutions and CsCl–NOM mixtures become less shielded with increasing CsCl concentration but are not affected by the presence of NOM.

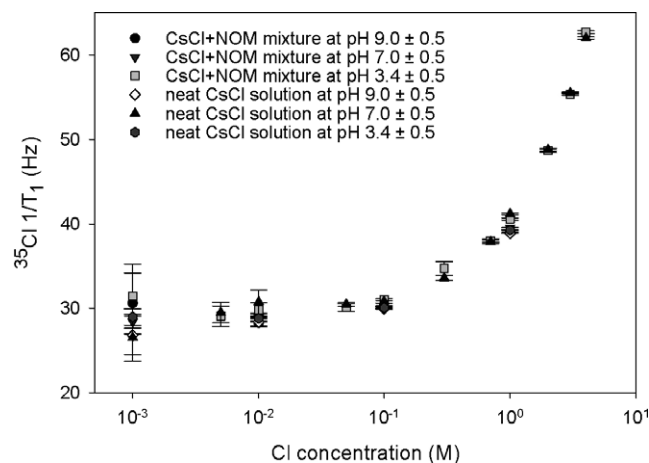


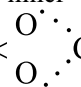
Fig. 6. ^{35}Cl NMR $1/T_1$ relaxation rates of CsCl solutions and CsCl–NOM mixtures increase with increasing CsCl concentration but are not affected by the presence of NOM.

3.2. Interpretation of ^{133}Cs and ^{35}Cl NMR chemical shifts and relaxation rates

Despite the absence of a significant effect of NOM on the ^{133}Cs chemical shifts, which by itself might suggest little Cs–NOM interaction, the ^{133}Cs $1/T_1$ relaxation data and FWHHs clearly demonstrate significant Cs–NOM association. Association of atoms or molecules in solution with a surface or large molecule typically decreases the reorientational frequency of the observed species, thus increasing its NMR $1/T_1$ relaxation rate (Mason, 1987). This is because the water reorientation frequencies in solution are typically of the order of 10^{10} Hz, and the decreased frequency near a surface or large molecule increases the intensity of the reorientational power spectrum at the Larmor frequency. This frequency is typically of the order of 10^8 Hz (78.67 MHz for ^{133}Cs at 600 MHz). T_1 relaxation is sensitive only to processes with significant Fourier components

in their power spectra at or near the Larmor frequency. This behavior has been used previously to investigate the interaction of ionic species with mineral surfaces (Kim et al., 1996b; Kim and Kirkpatrick, 1997, 1998; Yu and Kirkpatrick, 2001), but to our knowledge this is the first time it has been observed for metal–NOM interaction.

The observation of only a single, narrow, solution-like peak for the CsCl–NOM mixtures demonstrates that Cs⁺ is in rapid exchange between NOM-associated environments and bulk solution. If an observed species occupies two different types of structural environments statically, the NMR spectrum typically contains resolvable resonances representing those two environments. This is often the basis for mineral structure investigations using NMR. In contrast, if a species undergoes exchange between the two environments at a rate approximately an order of magnitude faster than the static peak width, only a single narrow resonance at the abundance-weighted average chemical shift is observed. Weiss et al. (1990) provide a more detailed discussion and examples involving exchange of Cs⁺ among different environments in clay interlayers. For the CsCl–NOM mixtures, the ¹³³Cs FWHHs increase systematically with decreasing [Cs], indicating increasing average 1/T₂ relaxation rates. This trend is the same as for the 1/T₁ relaxation rates. Under the conditions of rapid exchange observed here, the upper limit on the exchange rate is given by 1/τ = π · FWHH (Harris and Mann, 1978), where τ is the mean lifetime at each site. For the observed FWHH values of 22.7–9.9 Hz, the maximum lifetimes are 1.4 × 10⁻² to 3.2 × 10⁻² s, but they could be much shorter.

The lack of an NOM effect on the chemical shift of the dynamically averaged ¹³³Cs resonance indicates that the nearest neighbor chemical environments in the bulk solution and near the NOM are very similar. This observation is best interpreted to indicate that the NOM-associated Cs⁺ retains all or most of its shell of hydration water molecules and is associated with the NOM principally as outer sphere complexes. Previous studies of the effects of mineral surfaces on ¹³³Cs chemical shifts have shown a ca. 26–76 ppm deshielding for inner sphere Cs⁺ sorbed on kaolinite and illite (Kim et al., 1996b). NOM develops negative structural charge due principally to pH-dependent deprotonation of carboxylic (–COOH) and phenolic (–C₆H₅–OH) groups (Sposito, 1984). The SRNOM titration results show that for this material, carboxylic groups are the principal source of charge development and have pK_as of 4–5 and that phenolic groups with pK_as near 9 also contribute (Ritchie and Perdue, 2003). Thus, if Cs⁺ were strongly associated with the NOM as inner sphere complexes, at for instance bidentate –C <  Cs sites, it would have carboxyl O-atoms as nearest neighbors, and the chemical shift would be more positive, as for the clay surfaces. Our NMR data alone cannot distinguish whether the Cs⁺ occurs near the NOM as outer sphere complexes at specific sites or in the diffuse (Gouy) layer (Sposito, 1984; Kim and Kirkpatrick,

1997). The MD simulation results discussed below support the latter.

In contrast to the ¹³³Cs NMR results, the ³⁵Cl NMR chemical shifts, line shapes, and T₁ relaxation rates are unaffected by the presence of NOM except at [CsCl] > 2, demonstrating that there is no detectable complexation between Cl⁻ and NOM at any pH examined except perhaps at very high concentrations. This result is fully consistent with pH-dependent charge development on NOM described above. The negative structural charge of the NOM prevents significant close approach of the Cl⁻ and NOM, thus preventing any changes in local structural environment and relaxation rate. The contrasting behavior of the ¹³³Cs⁺ and ³⁵Cl⁻ ions in this system also indicates the absence of any co-adsorption effects at [CsCl] < 2 due to, e.g., formation of Cs–Cl ion clusters that could be associated with the NOM.

3.3. Extent of Cs⁺–NOM interaction

As for chemical shifts, 1/T₁ relaxation rates are abundance-weighted averages over the occupied sites under rapid exchange conditions. Two-site exchange models are often used to determine fractional site abundances from the observed 1/T₁ relaxation rates (Pfeifer, 1972; Kim and Kirkpatrick, 1998; Yu and Kirkpatrick, 2001; Rossi et al., 2003). In the simplest case of rapid 2-site exchange, the observed 1/T₁ relaxation rate would be the abundance-weighted sum of the rates in the bulk solution and near the NOM (Pfeifer, 1972; Kim and Kirkpatrick, 1998; Yu and Kirkpatrick, 2001):

$$1/T_{1,\text{obs}} = a/T_{1,\text{NOM}} + (1 - a)/T_{1,\text{sol}}, \quad (2)$$

where *a* is the fraction of the atoms associated with the NOM, (1 – *a*) is the fraction in the bulk solution, T_{1,obs} is the experimentally observed relaxation rate for the CsCl–NOM solutions, T_{1,NOM} is the relaxation rate of an atom associated with NOM, and T_{1,sol} is the experimentally determined relaxation rate of an atom in bulk solution. Unfortunately, for the CsCl–NOM mixtures, the observed ¹³³Cs 1/T₁ relaxation rates do not converge to a constant value representing 1/T_{1,NOM} at low concentrations. Thus, 1/T_{1,NOM} is unknown, and obtaining reliable, quantitative site abundances from Eq. (2) is not possible. Qualitatively, however, the trends of the observed 1/T₁ values (Fig. 2) suggest that the fraction of NOM-associated Cs⁺ increases with decreasing [Cs] at constant pH and with increasing pH at constant [Cs]. At a constant pH, the increase with decreasing [Cs] is due to the need for a larger fraction of the Cs⁺ to be associated with NOM to provide local charge balance. Since our solutions contained no background electrolyte, decreasing [Cs] also means decreasing total ionic strength, which would have the effect of increasing –COOH protonation and, thus, decreasing the amount of NOM-associated Cs⁺, opposite the observed trend. As discussed above,

the increase in Cs–NOM association with increasing pH results from the pH-dependent negative structural charge development due to increased deprotonation of acid sites with increasing pH (Sposito, 1984). For SRNOM, carboxylic groups with pK_a s near 4–5 and to a lesser extent phenolic groups with pK_a s near 9 play the dominant role (Ritchie and Perdue, 2003). Thus, the comparatively small extent of Cs–NOM association at low pH is due to $Cs^+ - H^+$ competition for the acid sites. Assuming $pK_a = 4.5$ for the carboxylic groups (Li et al., 1998), about 22% of them are deprotonated at pH 3.4, but essentially all of the phenolic groups remain protonated. Under these conditions, $[H^+] = 0.0004$ M, of the order of the lowest $[Cs]$ in our experiments. At pH 7, $[H^+]$ is negligible relative to $[Cs]$ in all our samples, and essentially all of the carboxylic groups are deprotonated, leading to the increased observed Cs–NOM association. At pH 9, about 15% of the phenolic groups are also deprotonated, leading to the even greater Cs–NOM association.

Conformational changes of NOM may also contribute to low Cs–NOM association at low pH. Humic substances are known to fold more under acid conditions than under alkaline conditions, resulting in lower surface area/volume ratios (Myneni et al., 1999). Thus, at pH 3.4 SRNOM may expose less surface area to the bulk solution than at higher pH values. Increased ionic strength (I) may also cause a smaller exposed NOM surface area/volume ratio and thus decreased Cs–NOM association. Relative size distribution measurements of NOM show that it is “elongated” at low I , but “coiled” at high I (Murphy et al., 1994; Wagoner and Christman, 1997).

3.4. Molecular modeling of CsCl–NOM interaction

MD modeling of the interaction of Cs^+ and Cl^- with NOM provides detailed, molecular scale insight into the structural and dynamical characteristics of these interactions and presents additional support for the interpretations of the NMR data. The simulated atom–atom radial distribution functions (RDFs, Fig. 7) and running coordination numbers (Fig. 8) show Cs^+ association with NOM as principally outer sphere complexes as well as decreasing Cs^+ –NOM association and increasing Cs^+ – Cl^- association with increasing CsCl concentration. In all cases the majority of nearest neighbors (NN) and next-nearest neighbors (NNN) to Cs^+ are water molecules, although there is detectable NN and NNN coordination of Cs^+ by O-atoms of the NOM at low $[Cs]$, and the number of contact (NN) and outer sphere (NNN separated by H_2O) Cs^+ – Cl^- ion pairs increases with increasing CsCl concentration in both NOM–CsCl and neat CsCl solutions. Among our simulated systems, the most extensive Cs^+ –NOM interaction occurs at the lowest $[Cs]$ concentration of 0.3 M, which corresponds to the system containing only the NOM molecule and 3 Cs^+ for charge balance. In this case, the Cs^+ ions are more strongly associated with the NOM molecule than at higher con-

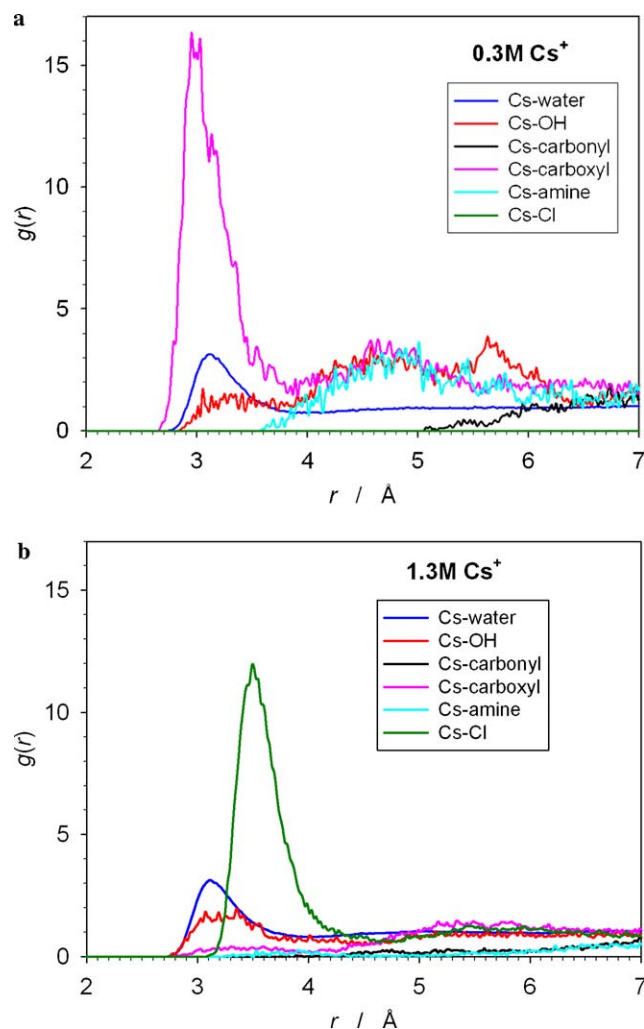


Fig. 7. MD-simulated radial distribution functions of Cs^+ ions with Cl^- (green) and H_2O (blue) in the solution and with NOM phenolic (red), carbonyl (black), carboxylic (pink), and amine (light blue) functional groups at two Cs^+ concentrations: 0.3 M (a) and 1.3 M (b).

centrations and remain in its vicinity throughout the simulation. At this concentration, on average each Cs^+ has ~ 8 NN H_2O , ~ 0.3 NN O-atoms of the deprotonated carboxylic groups, and ~ 0.1 NN O-atoms of phenolic and other alcohol – R–OH groups. None of the other functional groups contribute to Cs^+ –NOM binding. In the second coordination shell of Cs^+ at this concentration there are ~ 40 H_2O , ~ 1 O-atom of carboxylic groups, and ~ 1 O-atom of phenolic and other alcohol groups. At $[Cs]$ greater than 0.4–0.5 M, most of the Cs^+ is not associated with the NOM, and the average Cs^+ NN and NNN coordination shells are nearly identical to those of neat CsCl solutions.

The computed dynamical properties of Cs^+ are consistent with these structural interpretations. The computed Cs^+ diffusion coefficients are unaffected by the presence of NOM within computational error, except at 0.3 M $[Cs]$ where it is $\sim 30\%$ smaller than in the neat solutions due to its stronger association with the NOM molecule

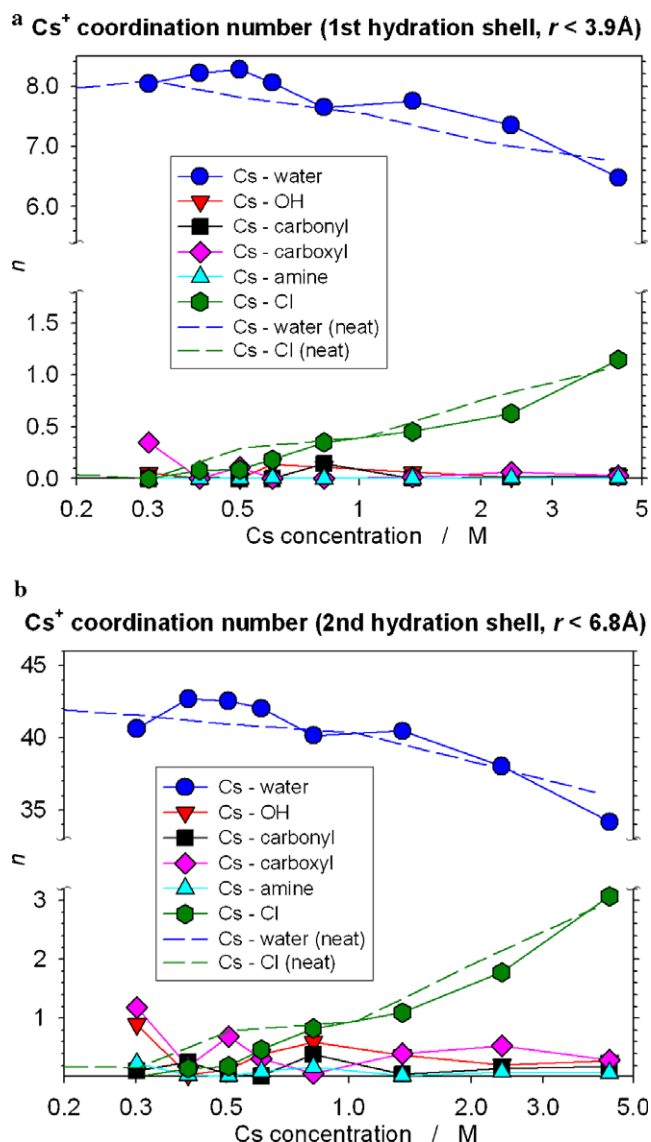


Fig. 8. MD-simulated contributions to the total number of neighbors in the first (a) and second (b) coordination shells of Cs^+ from various NOM functional groups and Cl^- and H_2O molecules as a function Cs concentration (note the logarithmic concentration scale and two different scales for the upper and lower parts of the plots).

(Fig. 9). The decreasing Cs^+ diffusion coefficients with increasing $[\text{Cs}]$ are due to increased Cs^+-Cl^- ion pairing.

The computed low-frequency dynamical power spectra of Cs^+ also show little effect of the presence of NOM except at the lowest $[\text{Cs}]$ (Fig. 10). The neat solutions show only a single feature near 20 cm^{-1} (Fig. 10b), which can be assigned to slow translational vibrations of the heavy Cs^+ ion in a weakly held hydration shell of H_2O molecules (e.g., Ohtaki and Radnai, 1993). The spectra for the CsCl-NOM systems also contain this 20 cm^{-1} band. In addition, for these systems spectral intensity grows in the $\sim 30\text{ cm}^{-1}$ range with decreasing $[\text{Cs}]$, and for the 0.3 M $[\text{Cs}]$ model there is a distinct band at this frequency. We have previously observed this feature (Fig. 10b) as a shoulder in the computed power

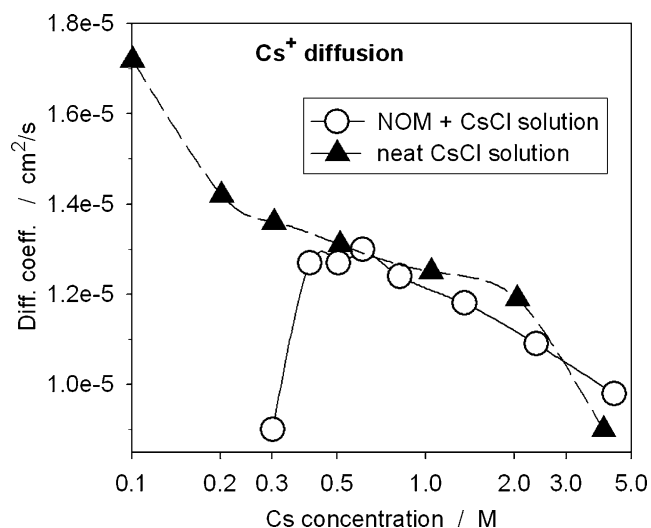


Fig. 9. MD-simulated diffusion coefficients of Cs^+ in CsCl-NOM aqueous solutions as a function of Cs concentration (note the logarithmic concentration scale). Symbol size corresponds to estimated statistical errors of the calculation.

spectrum of outer sphere Cs^+ associated with the neutral (001) surface of $\text{Ca}(\text{OH})_2$ (Kalinichev and Kirkpatrick, 2002) and as a more distinct peak for Cs^+ adsorbed as inner sphere complex on the siloxane (001) surface of kaolinite (Kalinichev and Kirkpatrick, unpublished results). This higher-frequency feature can be related to Cs^+ ions more strongly bound to their immediate environment, and thus can serve as an indicator of Cs^+-NOM association.

The computed structural and dynamical results for Cl^- show no effect of NOM on the Cl^- RDF, NN and NNN coordinations, diffusion coefficients or power spectra. The only change with increasing CsCl concentration is the increased association with Cs^+ described above, and this change occurs for both the neat and NOM solutions.

The MD modeling results strongly support the structural and dynamical interpretations of the ^{133}Cs and ^{35}Cl NMR data discussed above. The essentially outer sphere association of Cs^+ with the NOM is consistent with the experimental observation that NOM does not affect the ^{133}Cs chemical shift, since the computed average NN structure around Cs^+ is not greatly effected by this association. The greater occurrence of Cs^+ near the NOM at low concentrations and its decreasing average NOM association with increasing $[\text{Cs}]$ are also consistent with the experimentally observed increased ^{133}Cs $1/T_1$ relaxation rates at low $[\text{Cs}]$ and the convergence of these rates to those of the neat solutions at larger $[\text{Cs}]$. As discussed above, association with a surface or large molecule in solution reduces the average reorientation frequencies, increasing the intensity of the dynamical power spectrum at the resonance frequency and thus increasing the $1/T_1$ relaxation rate (Mason, 1987). Dynamically, the modest reduction in the Cs^+ diffusion coefficient due to NOM association is consistent with

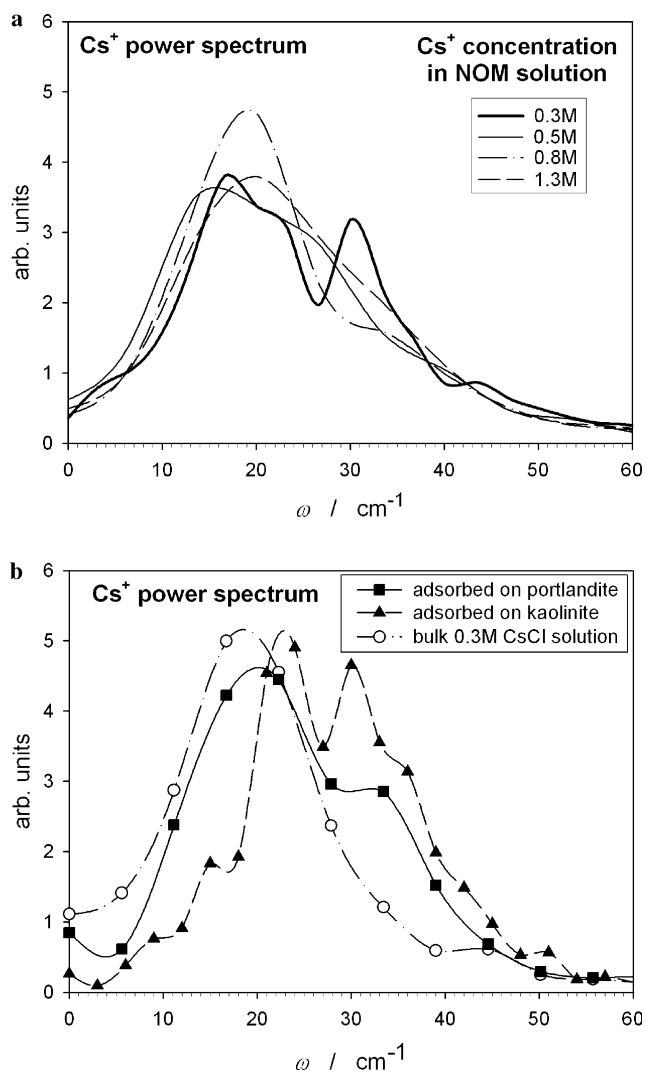


Fig. 10. Power spectra of Cs^+ translational dynamics: (a) in CsCl-NOM aqueous solutions as a function of Cs concentration; (b) for Cs^+ associated with the portlandite surface (squares), siloxane surface of kaolinite (triangles), and in the neat aqueous solution (circles).

the narrow, solution-like ^{133}Cs NMR resonances for all samples. Significant NMR line broadening would only occur if the rate of exchange between structural environments with different chemical shifts or the frequency of dynamical averaging of a quadrupolar line shape were reduced by orders of magnitude from those typical of aqueous solutions (e.g., Weiss et al., 1990).

4. Comparison to other systems

The occurrence of Cs^+ as outer sphere complexes associated with NOM is similar to the behavior of Na^+ adsorbed on silica gel, illite, kaolinite and boehmite, but contrasts with Cs^+ adsorbed on those phases. In these cases, surface Cs^+ readily occurs as inner sphere complexes (Kim et al., 1996b; Kim and Kirkpatrick, 1997, 1998). The difference may be due to the presence of relatively isolated carboxylic and phenolic groups on

the NOM compared to densely packed structural oxygens and hydroxyl groups on the mineral surfaces. The narrow, solution-like ^{133}Cs NMR line shapes indicate that Cs^+ undergoes dynamical exchange between NOM-associated sites and the bulk solution at frequencies greater than ca. 2.3×10^2 Hz. On the much shorter MD modeling time scale, the weak Cs^+ -NOM association can be detected by the presence of a spectral peak of translational vibrations in the solution at $\sim 30 \text{ cm}^{-1}$. This dynamical behavior is similar to that of Cs^+ and Na^+ on silica gel, illite, kaolinite and boehmite (Kim and Kirkpatrick, 1997) and also to Cl^- -associated with portlandite, Ca,Al layered double hydroxide, and the layer-structure hydrous Ca-silicates jennite and tobermorite (Kirkpatrick et al., 1999; Yu and Kirkpatrick, 2001; Kalinichev and Kirkpatrick, 2002; Kalinichev et al., 2006).

The interactions between dissolved ions and macromolecules in solution depend sensitively on the relative energies of the ions in bulk solution and in the bound state. There is now a developing body of experimental data that illustrates a range of possible types of interaction. Thallium (present as Tl^+) interacts quite strongly with the protein gramicidin A (present as dimers, Gr_2) dissolved in 2,2,2-trifluoroethanol (Turner et al., 1982). In this system, the ^{205}Tl chemical shifts change as much as 360 ppm as the Gr_2/Tl^+ ratio increases from 0 to about 0.2. Thermodynamic analysis of variable temperature NMR data combined with a 2-site exchange model indicate that Tl^+ is only partially solvated at the binding sites of the gramicidin A dimer channel (inner sphere complexes). This contrasts with our observation for Cs^+ -NOM, which suggest that NOM-associated Cs^+ in H_2O retains its hydration shell more completely. ^{113}Cd NMR data for $\text{SRNOM-Cd}(\text{ClO}_4)_2$ in D_2O at pD values from 3.6 to 9.0 and in Cd/C ratios from 0.0013 to 0.0068 show a strong pD effect on Cd-NOM complexation and a smaller effect of Cd/C ratio (Li et al., 1998). As for our ^{133}Cs spectra, there is only a single, narrow ^{133}Cd peak at acidic pD values. At higher pD values, however, the ^{133}Cd spectra contain a broader, more complex peak demonstrating a slower Cd exchange rate between bulk solution and NOM. The authors interpret this difference to be due to a larger concentration of “free” or uncomplexed Cd^{2+} at low pD than at high pD and probably increased coordination of Cd^{2+} by N-sites in the NOM at high pDs. For ^{51}V , which is present in solution as many different vanadate and poly-vanadate species, the interaction of these species with humic substance (HS) from Myall Lake, Australia, shows strong pH and concentration dependence (Lu et al., 1998). In contrast to our ^{133}Cs NMR spectra, the ^{51}V NMR spectra can exhibit more than one peak due to complex simultaneous protonation and oligomerization equilibria.

The trends of Cs^+ -NOM association observed in our study are also quite similar to the sorption of NOMs with

widely varying composition and structure onto goethite at approximately pH 4, as studied by batch sorption experiments (Kaiser, 2003). These results indicate interaction of negatively charged NOM with positively charged goethite surfaces, comparable to the interaction of NOM with dissolved Cs⁺ in our experiments. The total number of acidic groups attached to aromatic rings in the NOM positively and linearly controls the interaction between NOM and goethite.

Acknowledgments

This research was supported by DOE Basic Energy Sciences (Grant DEFGO2-00ER-15028) and the NSF Science and Technology Center of Advance Materials for Water Purification with Systems (WaterCAMPWS) at the University of Illinois. Computation was partially supported by the National Computational Science Alliance (Grant EAR 990003N) and utilized NCSA SGI/CRAY Origin 2000 computers and Cerius2-4.9 software package from Accelrys. We thank Xiaoqiang Hou and Randall T. Cygan for many useful discussions. The final paper benefited greatly from three anonymous reviews.

Associate editor: William H. Casey

References

- Aiken, G.R., Brown, P.A., Noyes, T.I., Pinckney, D.J. 1994. Molecular size and weight of fulvic and humic acids from the Suwannee River. In: Averett, R.C., Leenheer, J.A., McKnight, D.M., Thorn, K.A. (Eds.), *Humic Substances in the Suwannee River, Georgia: Interactions, Properties, and Proposed Structures*. US Geological Survey Water-Supply Paper 2373. pp. 89–97.
- Aiken, G.R., McKnight, D.M., Wershaw, R.L., MacCarthy, P., et al., 1985. *Humic Substances in Soil, Sediment, and Water: Geochemistry, Isolation, and Characterization*. John Wiley & Sons, Inc.
- Akitt, J.W., 1989. Multinuclear studies of aluminum compounds. *Prog. NMR Spectrosc.* **21**, 1–149.
- Allen, M.P., Tildesley, D.J., 1987. *Computer Simulation of Liquids*. Clarendon Press, Oxford.
- Berendsen, H.J.C., Postma, J.P.M., van Gunsteren, W.F., Hermans, J., 1981. Interaction models for water in relation to protein hydration. In: Pullman, B. (Ed.), *Intermolecular Forces*. Riedel, Dordrecht, The Netherlands, p. 331.
- Buffle, J., 1988. *Complexation Reactions in Aquatic Systems: an Analytical Approach*. Ellis Horwood Ltd.
- Bunzl, K., Puhakainen, M., Riekkinnen, I., Karhu, P., Schimmack, W., Heikinen, T., Jaakkola, T., Nikonov, V., Pavlov, V., Rahola, T., Rissanen, K., Suomela, M., Tillander, M., Ayras, M., 2001. Fallout ¹³⁷Cs, ⁹⁰Sr and ^{239,240}Pu in soils polluted by heavy metals: vertical distribution, residence half-times, and external gamma-dose rates. *J. Radioanal. Nucl. Chem.* **247**, 15–24.
- Conte, P., Piccolo, A., Lagen, B.V., Buurman, P., Hemminga, M.A., 2002. Elemental quantitation of natural organic matter by CPMAS ¹³C NMR Spectroscopy. *Solid State Nucl. Magn. Reson.* **21**, 158–170.
- Cygan, R.T., Kubicki, J.D. (Eds.), 2001. Molecular Modeling Theory and Applications in the Geosciences, *Reviews in Mineralogy and Geochemistry*, vol. **42**, Mineralogical Society of America, Washington, D.C.
- Dang, L.X., 1995. Mechanism and thermodynamics of ion selectivity in aqueous solutions of 18-crown-6 ether—a molecular dynamics study. *J. Am. Chem. Soc.* **117**, 6954–6960.
- Dang, L.X., Smith, D.E., 1993. Molecular dynamics simulations of aqueous ionic clusters using polarizable water. *J. Chem. Phys.* **99**, 6950–6956.
- Davies, G., Ghabbour, E.A., Cherkasskiy, A., Fatattah, A., 2001. Tight metal binding by solid phase peat and soil humic acids. In: Clapp, C.E. (Ed.), *Humic Substances and Chemical Contaminants*. Soil Science Society of America, pp. 371–395.
- Diallo, M.S., Simpson, A., Gassman, P., Faulon, J.-L., Johnson Jr., J.H., Goddard III, W.A., Hatcher, P., 2003. 3-D Structural modeling of humic acids through experimental characterization, computer-assisted structure elucidation and atomistic simulations. I. Chelsea Soil humic acid. *Environ. Sci. Technol.* **37**, 1783–1793.
- Elkins, K.M., Nelson, D.J., 2002. Spectroscopic approaches to the study of the interaction of aluminum with humic substances. *Coord. Chem. Rev.* **228**, 205–225.
- Fukushima, E., Roeder, S.B.W., 1981. *Experimental Pulse NMR: A Nuts and Bolts Approach*. Addison-wesley Publishing Company, Inc.
- Gaffney, J.S., Marley, N.A., Clark, S.B., 1996. Humic and fulvic acid and organic colloidal materials in the environment. In: *Humic and Fulvic Acids: Isolation, Structure and Environmental Role*, pp. 2–3, 8–10.
- Halliday J.D., Richards R.E., Sharp R.R., 1969. Chemical shifts in nuclear resonances of Caesium ions in solutions. In: *Proceedings of the Royal Society of London*, it Series A, *Mathematical and Physical Sciences* **313**, pp. 45–69.
- Hamilton-Taylor, J., Postill, A.S., Tipping, E., Harper, M.P., 2002. Laboratory measurements and modeling of metal-humic interactions under estuarine conditions. *Geochim. Cosmochim. Acta* **66**, 403–415.
- Harris, R.K., Mann, B.E., 1978. *NMR and the Periodic Table*. Academic Press, New York.
- Haynes, M.H.B., Clapp, C.E., 2001. Humic substances: considerations of compositions, aspects of structure, and environmental influences. *Soil Sci.* **166**, 723–737.
- Hinton, T.G., Knox, A., Kaplan, D., Serkiz, S., 2001. An in situ method for remediating ¹³⁷Cs contaminated wetlands using naturally occurring minerals. *J. Radioanal. Nucl. Chem.* **249**, 197–202.
- Hong, S.K., Elimelech, M., 1997. Chemical and physical aspects of natural organic matter (NOM) fouling of nanofiltration membranes. *J. Membr. Sci.* **132**, 159–181.
- Huber, C., Filella, M., Town, R.M., 2002. Computer modelling of trace metal ion speciation: practical implementation of a linear continuous function for complexation by natural organic matter. *Comput. Geosci.* **28**, 587–596.
- Kaiser, K., 2003. Sorption of natural organic matter fractions to goethite (alpha-FeOOH): effect of chemical composition as revealed by liquid-state ¹³C NMR and wet-chemical analysis. *Org. Geochem.* **34**, 1569–1579.
- Kalinichev, A.G., Kirkpatrick, R.J., 2002. Molecular dynamics modeling of chloride binding to the surfaces of calcium hydroxide, hydrated calcium aluminate, and calcium silicate phases. *Chem. Mater.* **14**, 3539–3549.
- Kalinichev, A.G., Wang, J., Kirkpatrick, R.J., 2006. Molecular dynamics modeling of the structure, dynamics and energetics of mineral-water interfaces: Application to cement materials, *Cement and Concrete Research*, in press.
- Kim, Y., Cygan, R.T., Kirkpatrick, R.J., 1996a. ¹³³Cs NMR and XPS investigation of cesium adsorbed on clay minerals and related phases. *Geochim. Cosmochim. Acta* **60**, 1041–1052.
- Kim, Y., Kirkpatrick, R.J., 1997. ²³Na and ¹³³Cs NMR study of cation adsorption on mineral surfaces: Local environments, dynamics, and effects of mixed cations. *Geochim. Cosmochim. Acta* **61**, 5199–5208.
- Kim, Y., Kirkpatrick, R.J., 1998. NMR T₁ relaxation study of ¹³³Cs and ²³Na adsorbed on illite. *Am. Mineral.* **83**, 661–665.
- Kim, Y., Kirkpatrick, R.J., Cygan, R.T., 1996b. ¹³³Cs NMR study of cesium on the surfaces of kaolinite and illite. *Geochim. Cosmochim. Acta* **60**, 4059–4074.

- Kirkpatrick, R.J., Yu, P., Hou, X., Kim, Y., 1999. Interlayer structure, anion dynamics, and phase transitions in mixed-metal layered hydroxides: Variable temperature ^{35}Cl NMR spectroscopy of hydro-talcite and Ca-aluminate hydrate (hydrocalumite). *Am. Mineral.* **84**, 1186–1190.
- Kirkpatrick, R.J., Kalinichev, A.G., Wang, J., Hou, X., Amonette, J.E., 2005. Molecular modeling of the vibrational spectra of interlayer and surface species of layered double hydroxides. In: Theo Klopogge J. (Ed.), *The Application of Vibrational Spectroscopy to Clay Minerals and Layered Double Hydroxides, CMS Workshop Lectures*, vol. 13, The Clay Minerals Society, Aurora, CO, pp. 239–285.
- Kitson, D.H., Hagler, A.T., 1988. Theoretical studies of the structure and molecular dynamics of a peptide crystal. *Biochemistry* **27**, 5246–5257.
- Kubicki, J.D., Apitz, S.E., 1999. Models of natural organic matter and interactions with organic contaminants. *Org. Geochem.* **30**, 911–927.
- Lee, S., Cho, J.W., Elimelech, M., 2005. Combined influence of natural organic matter (NOM) and colloidal particles on nanofiltration membrane fouling. *J. Membr. Sci.* **262**, 27–41.
- Leenheer, J.A., Brown, G.K., MacCarthy, P., Cabaniss, S.E., 1998. Models of metal binding structures in fulvic acid from the Suwannee River, Georgia. *Environ. Sci. Technol.* **32**, 2410–2416.
- Leenheer, J.A., Croué, J.P., 2003. Characterizing aquatic dissolved organic matter. *Environ. Sci. Technol.* **37**, 18A–26A.
- Li, J., Perdue, E.M., Gelbaum, L.T., 1998. Using Cadmium-113 NMR spectrometry to study metal complexation by natural organic matter. *Environ. Sci. Technol.* **32**, 483–487.
- Lide, D.R. (Ed.), 2004. *CRC Handbook of Chemistry and Physics*, 85th Ed. CRC Press, Boca Raton, FL, p.8-61.
- Lu, X., Johnson, W.D., Hook, J., 1998. Reaction of vanadate with aquatic humic substances: an ESR and ^{51}V NMR study. *Environ. Sci. Technol.* **32**, 2257–2263.
- Mao, J., Schmidt-Rohr, K., Xing, B., 2000. Structural investigation of Humic Substances using 2D solid-state nuclear magnetic resonance. In: Ghabbour, E.A., Davies, G. (Eds.), *Humic Substances: Versatile Components of Plants, Soil and Water*. Royal Society of Chemistry, Cambridge, pp. 83–89.
- Mason, J., 1987. *Multinuclear NMR*. Plenum Press, pp. 639.
- Murphy, E.M., Zachara, J.M., Smith, S.C., Phillips, J.L., Wietsma, T.W., 1994. Interaction of hydrophobic organic compounds with mineral-bound humic substances. *Environ. Sci. Technol.* **28**, 1291–1299.
- Myneni, S.C.B., Brown, J.T., Martinez, G.A., Meyer-Ilse, W., 1999. Imaging of humic substance macromolecular structures in water and soils. *Science* **286**, 1335–1337.
- Ohtaki, H., Radnai, T., 1993. Structure and dynamics of hydrated ions. *Chem. Rev.* **93**, 1157–1204.
- Oliver, B.G., Thurman, E.M., Malcolm, R.L., 1983. The contribution of humic substances to the acidity of colored natural waters. *Geochim. Cosmochim. Acta* **47**, 2031–2035.
- Peña-Méndez, E.M., Gajdošová, D., Novotná, K., Prošek, P., Havel, J., 2005. Mass spectrometry of humic substances of different origin including those from Antarctica—a comparative study. *Talanta* **67**, 880–890.
- Perminova, I.V., Frimmel, F.H., Kudryavtsev, A.V., Kulikova, N.A., Abbt-Braun, G., Hesse, S., Petrosyan, V.S., 2003. Molecular weight characteristics of humic substances from different environments as determined by size exclusion chromatography and their statistical evaluation. *Environ. Sci. Technol.* **37**, 2477–2485.
- Pfeifer, H., 1972. Nuclear magnetic resonance and relaxation of molecules adsorbed on solids. In: Diehl, P., Fluck, E., Kosfeld, R. (Eds.), *NMR, Basic Principles and Progress*, vol. 7. Springer-Verlag, New York, pp. 53–153.
- Piccolo, A., 2001. The supramolecular structure of humic substances. *Soil Sci.* **166**, 810–832.
- Porquet, A., Bianchi, L., Stoll, S., 2003. Molecular dynamic simulations of fulvic acid clusters in water. *Colloids and Surfaces A-physicochem. Eng. Aspects* **217**, 49–54.
- Pullin, M.J., Cabaniss, S.E., 2003. The effects of pH, ionic strength, and iron–fulvic acid interactions on the kinetics of non-photochemical iron transformations. I. Iron(II) oxidation and iron(III) colloid formation. *Geochim. Cosmochim. Acta* **67**, 4079–4089.
- Ritchie, J.D., Perdue, E.M., 2003. Proton-binding study of standard and reference fulvic acids, humic acids, and natural organic matter. *Geochim. Cosmochim. Acta* **67**, 85–96.
- Rossi, S., Luckham, P.F., Green, N., Cosgrove, T., 2003. NMR solvent relaxation studies of Na^+ -montmorillonite clay suspensions containing non-ionic polymers. *Colloids Surf. A: Physicochem. Eng. Aspects* **215**, 11–24.
- Ruhm, W., Konig, K., Bayer, A., 1999. Long-term follow-up of the ^{137}Cs body burden of individuals after the Chernobyl accident—a means for the determination of biological half-lives. *Health Phys.* **77**, 373–382.
- Schlick, T., 2002. *Molecular Modeling and Simulation—An Interdisciplinary Guide*. Springer-Verlag, New York, p. 634.
- Schulten, H.R., Schnitzer, M., 1997. Chemical model structures for soil organic matter and soils. *Soil Sci.* **162**, 115–130.
- Sein Jr., L.T., Varnum, J.M., Jansen, S.A., 1999. Conformational modeling of a new building block of humic acid: Approaches to the lowest energy conformer. *Environ. Sci. Technol.* **33**, 546–552.
- Shevchenko, S.M., Bailey, G.W., Akim, L.G., 1999. The conformational dynamics of humic polyanions in model organic and organo-mineral aggregates. *J. Mol. Struct. (Theochem)* **460**, 179–190.
- Simpson, A.J., Kingery, W.L., Hayes, M.H.B., Spraul, M., Humpfer, E., Dvortsak, P., Kerssebaum, R., Godejohann, M., Hofmann, M., 2002. Molecular structures and associations of humic substances in the terrestrial environment. *Naturwissenschaften* **89**, 84–88.
- Sposito, G., 1981. Trace metals in contaminated waters. *Environ. Sci. Technol.* **15**, 396–403.
- Sposito, G., 1984. *The Surface Chemistry of Soils*. Oxford University Press, Inc.
- Struyk, Z., Sposito, G., 2001. Redox properties of standard humic acids. *Geoderma* **102**, 329–346.
- Sutton, R., Sposito, G., Diallo, M.S., Schulten, H.R., 2005. Molecular simulation of dissolved organic matter. *Environ. Toxicol. Chem.* **24**, 1902–1911.
- Swift, R.S., 1999. Macromolecular properties of soil humic substances: Fact, fiction, and opinion. *Soil Sci.* **164**, 790–802.
- Tegen, I., Door, H., Munnich, K.O., 1991. Laboratory experiments to investigate the influence of microbial activity on the migration of cesium in a forest soil. *Water Air Soil Pollut.* **57–58**, 441–447.
- Thiry, Y., Myttenaere, C., 1993. Behaviour of radio-caesium in forest multilayered soils. *J. Environ. Radioact.* **18**, 247–257.
- Tipping, E., Rey-Castro, C., Bryan, S.E., Hamilton-Taylor, J., 2002. Al (III) and Fe (III) binding by humic substances in freshwaters, and implications for trace metal speciation. *Geochim. Cosmochim. Acta* **66**, 3211–3224.
- Turner, G.L., Hinton, J.F., Millett, F.S., 1982. A thallium-205 NMR study of the thallium(I)-gramicidin A association in trifluoroethanol. *Biochemistry* **21**, 646–651.
- Valcke, E., Cremers, A., 1994. Sorption-desorption dynamics of radio-caesium in organic matter soils. *Sci. Total Environ.* **157**, 275–283.
- Wagoner, D.B., Christman, R.F., 1997. Molar mass and size of Suwannee River natural organic matter using multi-angle laser light scattering. *Environ. Sci. Technol.* **31**, 937–941.
- Walling, D.E., Quine, T.A., 1991. Use of ^{137}Cs measurements to investigate soil-erosion on arable fields in the UK—Potential applications and limitations. *J. Soil Sci.* **42**, 147–165.
- Wang, J., Kalinichev, A.G., Amonette, J.E., Kirkpatrick, R.J., 2003. Interlayer structure and dynamics of Cl-bearing hydro-talcite: Far

- infrared spectroscopy and molecular dynamics modeling. *Am. Mineral.* **88**, 398–409.
- Weiss, C.A.J., Kirkpatrick, R.J., Altaner, S.P., 1990. The structural environments of cations adsorbed onto clays: ^{133}Cs variable-temperature MAS NMR spectroscopic study of hectorite. *Geochim. Cosmochim. Acta* **54**, 1655–1669.
- Wershaw, R.L., 1999. Molecular aggregation of humic substances. *Soil Sci.* **164**, 803–813.
- Wershaw, R.L., Aiken, G.R., Leenheer, J.A., Tregellas, J.R., 2000. Structural-group quantitation by CP/MAS ^{13}C NMR measurements of dissolved organic matter from natural surface waters. In: Ghabbour, E.A., Davies, G. (Eds.), *Humic Substances: Versatile Components of Plants, Soil and Water*. Royal Society of Chemistry, Cambridge, pp. 63–81.
- Yu, P., Kirkpatrick, R.J., 2001. ^{35}Cl NMR relaxation study of cement hydrate suspensions. *Cement Concrete Res.* **31**, 1479–1485.